TECHNICAL MEMORANDUM

272

The ECMWF operational implementation of four dimensional variational assimilation. Part II: Experimental results with improved physics

J-F. Mahfouf and F Rabier

Research Department

February 1999

European Centre for Medium-Range Weather Forecasts
Europäisches Zentrum für mittelfristige Wettervorhersage
Centre européen pour les prévisions météorologiques à moyen

The ECMWF operational implementation of four dimensional variational assimilation Part II: Experimental results with improved physics

By **J.-F. Mahfouf and F. Rabier**

Abstract

A comprehensive set of physical parametrizations has been linearized for use in the experimental ECMWF 4D-Var system described in Part I. The following processes are represented : vertical diffusion, sub-grid scale orographic effects, large scale precipitation, deep moist convection and longwave radiation. The tangent-linear approximation is examined for finite-size perturbations. Significant improvements are illustrated for surface wind and specific humidity with respect to a simplified vertical diffusion scheme. Singular vectors computed over 6 hours (compatible with the 4D-Var assimilation window) have lower amplification rates with the improved physical package due to a better description of dissipation processes. However, latent heat release contributes to amplify the potential energy of perturbations in rainy areas. A direct consequence of these results is a larger observation term of the cost-function in the minimization process when improved physics is included in 4D-Var. The larger departure of the analysis state to observations for the lower resolution problem is in better agreement with the behaviour of the full non-linear model at high resolution. The expensive cost of the linear physics has required to define a new configuration of the incremental 4D-Var system with two outer loops. A first minimization is performed at low resolution with simplified physics (50 iterations) followed by a second minimization with improved physics (20 iterations) after an update of the model trajectory at high resolution. In such configuration the extra-cost of the physics is only 25 % and positive impacts are shown in terms of quality of the forecasts in the tropics (reduced spin-down of precipitation, lower errors in wind scores). This 4D-Var configuration with improved physics is extensively evaluated against 3D-Var in Part III of this series of papers.

1. INTRODUCTION

In the first part of this series of three papers, preliminary results on the first operational four-dimensional variational (4D-Var) assimilation at ECMWF (European Centre for Medium Range Weather Forecasts) were described (Rabier et al., 1999). A first configuration using almost adiabatic tangent-linear and adjoint models over a 6-hour assimilation window has been compared to the ECMWF operational 3D-Var assimilation system (Courtier et al., 1998; Rabier et al., 1998b; Andersson et al., 1998), with a better overall performance of the 4D-Var system. An incremental approach, as proposed by Courtier et al. (1994), has been chosen with one outer- loop and an "operational" resolution T213L31/T63L31.

Part II focuses on improving the linear versions of the ECMWF model through the inclusion of physical parameterizations schemes. Linearized physical processes should improve the time evolution of analysis increments and the estimation of the gradient of the cost-function with respect to the model initial state. They are expected to be important near the surface through momentum friction and in tropical regions where the large scale circulation is mostly driven by diabatic heating. Physical processes also need to be linearized in order to include new types of observations related to the hydrological cycle (precipitation, cloud cover, cloud water and ice contents, ...) in variational data assimilation systems. Introducing physical processes in linear models is not trivial since most of them are strongly non-linear and include on/off switches. However, preliminary encouraging results have been obtained by various authors (Zou et al., 1993; Zupanski, 1993; Zou, 1996; Tsuyuki, 1996). For operational applications a trade-off is necessary between the expensive cost of the linearized physics and the benefit it can provide in terms of quality of analyses and forecasts.

Section 2 describes a first set of linearized physical parameterizations developed for the ECMWF model. Necessary simplifications with respect to the operational non-linear physical package are explained. Section 3 examines how the linear physics does actually improve the tangent-linear approximation for propagating analysis increments over a 6-hour window. Singular vectors produced with an adiabatic model are compared to those produced with the linear physics.

Section 4 presents preliminary 4D-Var experiments performed over few cycles in order to define a first optimal configuration with linear physics. Results from a 4D-Var incremental assimilation with two outer-loops including physical processes in the second minimization are compared in Section 5 to an adiabatic configuration of 4D-Var. The main results are summarized in Section 6.

2. DESCRIPTION OF THE LINEAR PHYSICS

A set of linearized physical processes has been developed at ECMWF for singular vector computation (Buizza, 1994), sensitivity studies (Klinker et al., 1998) and 4D-Var assimilation (Rabier et al., 1998a). The strategy adopted is described in details by Mahfouf et al. (1996) and Mahfouf (1998). A number of simplifications have been defined with respect to the operational non-linear physical parametrizations. The main feedback loops between the processes are described except for cloud-radiation interactions which will require important future developments. Some simplifications have been designed to avoid spurious positive feedback loops in the linearized versions, that the lack of non-linear interactions cannot prevent from growing with time.

2.1 Vertical diffusion

A vertical diffusion scheme based on a K-type closure with exchange coefficients depending upon the local Richardson number *Ri* as described in Louis et al. (1982) is adopted. Analytical expressions are generalized to the situation of different roughness lengths for heat and momentum transfers. The mixing length profile $l(z)$ uses the formulation of Blackadar (1962) with a reduction in the free atmosphere. For any conservative variable ψ (wind components u,v ; dry static energy s ; specific humidity q), the tendency of its perturbation ψ' produced by vertical diffusion is :

$$\frac{\partial \psi'}{\partial t} = \frac{1}{\rho}\frac{\partial}{\partial z}\left(K(Ri)\frac{\partial \psi'}{\partial z}\right) \tag{1}$$

where ρ is the air density.

The exchange coefficient K is given by the following expression:

$$K = l^2\left|\frac{\partial \vec{V}}{\partial z}\right| f(Ri) \tag{2}$$

where $\vec{V}$ is the wind vector. The analytical expressions for $f(Ri)$ are given in Louis et al. (1982). In Equation (1), perturbations of the exchange coefficients are neglected ($K'=0$).

2.2 Subgrid-scale orographic effects

The low level blocking part of the scheme developed by Lott and Miller (1997) is represented in the linear scheme. The tendency for wind perturbations $\vec{V}'$ produced by the low level drag processes is

$$\frac{\partial \vec{V}'}{\partial t} = \frac{1}{\rho}\frac{\partial \vec{\tau}'}{\partial z} \tag{3}$$

where $\vec{\tau}'$ is the perturbation in momentum flux

2.3 Large-scale precipitation

A linearized version of a local moist adjustment scheme designed to produce stratiform precipitation has been chosen instead of the current ECMWF prognostic cloud scheme (Tiedtke, 1993).

If (q,T) is an initial supersaturated state $(q>q_s(T))$, a final adjusted state (q^*,T^*) such that $q^*=q_s(T^*)$ is obtained by conserving moist static energy in a given atmospheric layer. The adjusted values are obtained through an iterative method with two updates.

The equations for the non-linear scheme are :

$$\begin{aligned} T^* - T &= -\lambda(q_s(T^*) - q) \\ q^* - q &= q_s(T^*) - q \end{aligned} \tag{4}$$

with $\lambda = L/C_p$, where L is the latent heat of liquid water and C_p is the specific heat at constant pressure.

The above equations are solved from a linearization of the specific humidity at saturation $q_s(T^*) = q_s(T) + \gamma(T^* - T)$ with $\gamma = (\partial q_s)/(\partial T)$. Then, the linearization of $q_s(T')$ as $\gamma \times T'$ provides the equations for the tangent-linear scheme:

$$\begin{aligned} T'^* - T' &= \frac{-\lambda}{1+\lambda\gamma}(\gamma \times T' - q') \\ q'^* - q' &= \frac{1}{1+\lambda\gamma}(\gamma \times T' - q') \end{aligned} \tag{5}$$

Tendencies produced by large-scale condensation are thus :

$$\frac{\partial q'}{\partial t} = -\frac{1}{\lambda}\frac{\partial T'}{\partial t} = \frac{q'^* - q'}{2\Delta t} \tag{6}$$

where Δt is the model time step.

This scheme also accounts for melting of snow whenever the temperature of a given layer exceeds 2^0C. Evaporation of precipitation in subsaturated layers is strongly reduced with respect to the non-linear scheme in order to avoid the growth of non-meteorological singular vectors as explained in Mahfouf (1998).

2.4 Deep moist convection

The physical tendencies produced by convection on any conservative variable ψ can be written in a mass-flux formulation as (see Betts, 1997):

$$\frac{\partial \psi}{\partial t} = \frac{1}{\rho}\left[(M_u + M_d)\frac{\partial \psi}{\partial z} + D_u(\psi_u - \psi) + D_d(\psi_d - \psi)\right] \tag{7}$$

The first term on the right hand side represents the compensating subsidence induced by cumulus convection on the environment through the mass-flux M. The other terms account for the detrainment of cloud properties in the environment via a detrainment rate D. The subscripts u and d refer to the updrafts and downdrafts properties respectively. Evaporation of cloud water and of precipitation should also be added in Equation (7) for s and q variables. Mass flux theory predicts that the effect of convection on large-scale temperature and moisture structures is dominated by compensating subsidence,

as shown for exemple in the study of Gregory and Miller (1989). Therefore, non-linear tendencies produced by convection can be approximated by:

$$\frac{\partial \psi}{\partial t} \approx \frac{1}{\rho}\left[(M_u + M_d)\frac{\partial \psi}{\partial z}\right] \tag{8}$$

This approximation is better for the heat budget than for the moisture budget (Betts, 1997). As a consequence, a partial linearization of Equation (8) is performed, where the vertical transport by the mean mass-flux is applied to the perturbations. From a non-linear integration of the ECMWF convection scheme (Tiedtke, 1989), mass-flux profiles $M(z)$ are computed to estimate the vertical transport of the perturbed variables ψ' :

$$\frac{\partial \psi'}{\partial t} = \frac{1}{\rho}\left[(M_u + M_d)\frac{\partial \psi'}{\partial z}\right] \tag{9}$$

This linearized equation only applies for deep convection. Indeed, for shallow convection, detrainement rates cannot be neglected in the estimation of the total tendencies. The justification for such linear convection scheme is based on previous use of simplifed physics at ECMWF. The experience with vertical diffusion for singular vectors (Buizza, 1994) has demonstrated that simplified physical parameterizations can improve the realism of a tangent-linear model, even if only part of the processes are described. The linear scheme developed by Buizza (1994) accounts only for neutral stability effects and uses a constant depth for the boundary layer, but is efficient enough to produce realistic momentum dissipation near the surface. Preliminary 4D-Var experiments by Rabier et al. (1998a) have also demonstrated that it is possible to improve the analysis of specific humidity by relaxing, in linearized models, the mean vertical velocity towards zero in the tropical belt. These encouraging results indicates that it is possible to describe the effect of cumulus induced subsidence in a more physical way with potential impact on 4D-Var. The present simplified linearized scheme must be seen as a first step before handling the complexity of the full operational ECMWF scheme. Results described in the next sections will demonstrate a posteriori that such simple scheme can improve significantly the time evolution of analysis increments in tropical regions.

2.5 Longwave radiation

Radiative transfer for the longwave spectrum is modeled using a constant emissivity formulation which was previously developed in the operational ECMWF forecast model to reduce the cost of radiative computations. This approach requires the storage of effective emissivity arrays ε computed from the full non-linear radiation scheme (Morcrette, 1990). Effective emissivity is defined in terms of the irradiance F and the local temperature T :

$$\varepsilon = \frac{F}{\sigma T^4} \tag{10}$$

where σ is the Stefan-Boltzmann constant.

The tendency of the perturbed temperature T' can thus be written:

$$\frac{\partial T'}{\partial t} = -\alpha \frac{g}{C_p}\frac{\partial}{\partial p}(4\varepsilon\sigma T^3 T') \tag{11}$$

with:

$$\alpha = \frac{1}{1+\left(\frac{p_r}{p}\right)^{10}} \tag{12}$$

in order to reduce the radiative tendencies above p_r=300 hPa (approximatively in the stratosphere). Equation (11) implies that the net longwave radiation at any level strongly depends on the temperature at that level. This is a reasonable approximation for optically thick atmospheres. In the stratosphere, as already stated by Thuburn (1994), the net longwave irradiance depends most strongly on conditions far below in the troposphere. It has been shown in Mahfouf (1998) that the emissivity method is unstable in the stratosphere. Therefore, the use of the linear longwave scheme is restricted to the troposphere. A proper consideration of cloud-radiation interactions will require the development of a simple radiation scheme that could be called at every model time step (instead of every three hours in the current operational model).

3. BEHAVIOUR OF THE LINEAR PHYSICS

3.1 Tangent-linear approximation

Analysis increments evolved with a tangent-linear version of the ECMWF global spectral model are compared with differences of non-linear (NL) integrations with the model including a full physical package. The goal of this study is to demonstrate that when including physical processes in the tangent-linear model its behaviour is in better agreement with the non-linear model. Similar comparisons have already been done by Mahfouf (1998) with a T42L31 version of the ECMWF model for 24-hour simulations. We present here a study at a higher horizontal resolution (T63) and over a time window of 6 hours compatible with the framework of 4D-Var experimentation.

Figure 1a displays analysis increments for the zonal wind at the lowest model level (~ 30 m above the surface) over the Northern Hemisphere. This level has been chosen since turbulent processes are dominant close to the surface. The increments are computed from the operational 3D-Var system (5 December 1996 at 00Z) and have values around 1ms^{-1}. Larger values are noticed over ocean areas where SHIP and BUOY surface winds observations are assimilated. Maximum values can reach up to 5 ms^{-1}. Given the fact that the tangent-linear approximation is supposed to be valid only for infinitesimal perturbations, testing the propagation of analysis increments consists in a rather severe evaluation. However, linear models can only be useful for variational data assimilation if they can provide a reasonable description of the evolution of finite-size perturbations. This has been demonstrated for adiabatic models (Lacarra and Talagrand, 1988) but only few studies have been performed with linear diabatic models (Janiskova et al., 1998; Errico and Raeder, 1998). The analysis increments evolved non-linearly are strongly reduced after 6 hours (Figure 1b). The higher surface drag over continents implies that the only non negligible values appear over the Atlantic and Pacific oceans. Even over the oceans the initial perturbations are reduced by a factor of two or three through momentum friction.

Figure 2 shows the tangent-linear evolutions obtained with two versions of the linear model. The first version, almost adiabatic and refered hereafter as Simplified Physics (SP), only represents surface drag and vertical diffusion assuming a neutral boundary layer as described in Buizza (1994). This simplified physics was used in the tangent-linear and adjoint models presented in Part I. The second version includes the physical parametrization schemes described in Section 2 and is refered hereafter as Improved Physics (IP). Although the 6-hour evolution with SP has significantly reduced the size of the initial increments (Figure 2a), they appear to be overestimated with respect to the non-linear reference (Figure 1b). This is particularly true over continents where momentum dissipation in clearly too weak with SP. This can be understood by the low value of surface roughness length (5 cm) chosen in the simplified vertical diffusion scheme. This leads to an underestimation of the surface stress around 0.5 Nm^{-2} over most of the continents. Figure 2b shows that the evolution produced using IP is in much better agreement with the NL evolution. Increments are very small over continents, they are also reduced over the Western Pacific (Kuroshio current) where strong unstable conditions prevail. The blocking effect of

the sub-grid scale orography scheme also acts to reduce low level wind speed near high mountain ranges with IP. Over the Atlantic ocean not significant differences are observed between SP and IP. Since the most spectacular differences between SP and IP take place over land where no SYNOP wind observations are used in the ECMWF data assimilation system (mostly due to representativeness problems) it is likely that this positive impact of the improved physics will not be reflected in terms of quality of the analyses for this atmospheric variable.

In order to get a more global view of the improvement coming from the linear physical package, the zonal mean of the mean absolute error in specific humidity is shown on Figure 3. The global error with IP compared to the NL evolution is 0.055 gkg^{-1} and is 0.065 gkg^{-1} with SP. Largest errors are located in the lowest equatorial troposphere. The inclusion of IP in the tangent-linear model improves the evolution of specific humidity increments in the boundary layer, since the simple vertical diffusion scheme of Buizza (1994) does not apply on moisture. Large reduction of the errors are also noticed at mid-latitudes where the large-scale condensation scheme is active in baroclinic disturbances. The inclusion of a simplified linear convection scheme improves the behaviour of the lower troposphere in the tropics. However, there is a slight degradation higher up where detrainement effects make the assumption of the dominance of the mass-flux transport used to derive Equation (9) less valid.

Conclusions obtained when comparing tangent-linear evolutions of analysis increments with non-linear evolutions are very similar to those presented by Mahfouf (1998) with a lower resolution model and over a longer time integration. It appears that even after a 6-hour evolution of analysis increments the tangent-linear approximation can be improved when diabatic processes are described. The improvement with respect to SP is noticable near the surface where momentum dissipation is more active (stability effects on turbulent transfers, low level blocking by sub-grid scale orography). Moist processes (large-scale condensation and deep convection) lead to significant improvements of evolved increments for specific humidity.

3.2 Singular vectors

Singular vectors were computed over a 6-hour window with a T63L31 of the ECMWF model for one of the intensive period of the field campaign FASTEX (IOP7 : 7 February 1997). Although the usual period to compute singular vectors is 48 hours, such comparison allows to examine how optimal perturbations can grow over the assimilation window of the 4D-Var configuration and to examine if the linear physics produces both different amplification rates and geographical locations with respect to adiabatic singular vectors. The spectrum of amplification factors for the first 16 singular vectors is presented on Figure 4 for both SP and IP. They have been computed over the Northern Hemisphere extra-tropics (above 30°N). Although a moist energy norm could have been used for the computation of growth rates (Mahfouf et al., 1996; Ehrendorfer et al.,1998) we have chosen here a dry energy norm to isolate the effects of diabatic processes in the linearized models. Apart from the first singular vector, the amplification factors are lower with IP than with SP in agreement with the increased dissipation produced by both the stability-dependent vertical diffusion scheme and the sub-grid scale orographic scheme. The projection of the first 10 singular vectors obtained with IP on the first 10 singular vectors obtained with SP leads to a 73 % similarity of the two sub-spaces, which means that the improved physics does not strongly modify the structure of the most unstables perturbations. This can be seen more clearly when examining the first singular vector evolved after 6 hours and located in the middle of the Atlantic ocean. It is depicted for temperature around 500 hPa (model level 15) on Figure 5 and for specific humidity near 700 hPa (model level 22) on Figure 6. For temperature, evolved singular vectors with SP and IP have a similar wave train pattern, with maxima and minima located about the same place, although the amplitude of the perturbations is somewhat larger with diabatic processes. With improved physics, kinetic energy is reduced by turbulent processes whereas potential energy is increased through latent heat release. However, potential energy is only 5 % of the total energy at optimization time. The effect of moist processes can be examined on Figure 6 where specific humidity perturbations are much larger with IP and also present different patterns (the negative anomaly along the 50 °N parallel with SP is almost inexistent with IP). Latent heat release is the mechanism by which static stability is reduced in baroclinic systems leading to higher growth rates of unstable modes.

The extra-tropical singular vectors using IP have a high degree of similarity with the singular vectors obtained with SP. This result is not surprising since the growth rate of such unstable modes is governed by the baroclinic instability which is essentially a dynamical process accurately described by adiabatic models. It appears that the amplification rates are lower with IP due to more active dissipative processes, which are in better agreement with the full non-linear model, as previously shown. However, latent heat release amplifies the potential energy component of the total energy. This result can be made more obvious when using a moist energy norm including both perturbations of temperature and specific humidity. The amplification rates are then systematically larger when moist processes are included in the linear models (Mahfouf et al., 1996 ; Ehrendorfer et al., 1998). In terms of data assimilation, it is likely that the fit to the data will be more difficult using IP that SP. This could be different in precipitating areas where latent heat release amplifies temperature perturbations. However, current assimilation systems do not use data in cloudy and rainy areas, it is therefore likely that the observed differences on the behaviour of singular vectors with the improved physics will not affect significantly the 4D-Var analyses in the extra-tropics.

4. Design of a 4D-Var configuration with physics

The first experimentation with 4D-Var assimilation including the linear physical processes was undertaken with a one outer-loop configuration. Three configurations where tested over few assimilation cycles starting from the 17 February 1997 at 00 Z. The first configuration corresponds to the standard 4D-Var sytem described in Part I which is almost adiabatic but still includes a very simple vertical diffusion scheme without stability effects (SP). A second configuration of 4D-Var includes the linear physics previously described and evaluated (IP). A last 4D-Var configuration corresponds to experiments run with full adiabatic tangent-linear and adjoint models (refered as AD). From these three experiments the progressive impact of including physical processes in the 4D-Var system is evaluated. The main lesson we learned from this exercise concerned the influence of physical processes on the convergence of the minimization, whereas the forecasts run from these three analyses did not show significant differences for improving a rapid cyclogenesis developing over Western Europe (IOP17 from FASTEX experiment).

The evolution of the cost-function for the observation term is presented for the 6-hour cycle around 17/02/1997 at 12 Z for the three 4D-Var configurations on Figure 7 together with the norm of the gradient. The convergence process is very similar between the three experiments, a minimum being reached in about 50 iterations (Figure 7a). Around iteration 30, the variational quality control is activated leading to the rejection of some data and therefore to a reduction of the cost-function. The norm of the gradient decreases by four orders of magnitude which is also an indication that the physics do not lead to convergence problems (Figure 7b). It is important to recognize that previous 4D-Var experiments with physics published in the litterature (Zou, 1993, Zupanski, 1993, Tsuyuki, 1996) where not performed with the incremental approach. In the incremental approach, the full problem is linearized around the background state and the actual problem to be minimized is quadratic. Therefore, convergence problems pointed out by various authors cannot take place in the inner loop of the incremental 4D-Var. However, it is interesting to notice on Figure 7a that the value of the cost-function reached at the minimum is the lowest with the AD configuration and the highest with the IP configuration. The fit to the observations is therefore easier with an adiabatic model since only dynamical constraints are imposed to the time evolution of increments. For example, as shown in the singular vector study, the growth rate of unstable perturbations is higher when the model contains only simplified physics which indicates that the improved linear physics is more dissipative. As a consequence, larger initial increments would be required with improved physics to fit observations in the middle of the assimilation window. In fact, the background term imposes similar size of analysis increments leading to a larger departure from the observations when the improved physics is included in 4D-Var.

The various terms of the cost-function at the minimum are depicted on Figure 8 for the low resolution problem (inner loop). The observation term is also presented for the high resolution problem (outer loop). The background and penality terms are very similar between the 4D-Var configurations but do not represent the major contribution to the total cost-

function. The mismatch between the observation term at low and high resolutions shows up the level of inconsistency in the incremental approach between the problem to be solved and the linear problem actually solved. An interesting feature of the 4D-Var configuration with improved physics is that the jump imposed when going from the low to the high resolution is smaller than for the configuration with simplified physics or without physics. As a consequence, the background term is larger for the AD configuration. Therefore, the better convergence of the low resolution adiabatic problem is produced by finding a low resolution model trajectory that "over-fits" the observations, which is somewhat in contradiction with the behaviour of the high resolution non-linear model. This result indicates that the inclusion of physical processes in 4D-Var provides a better consistency between the inner and outer loops of the incremental approach. The positive impact of the linear physics on the convergence of the incremental 4D-Var must be counterbalanced by the fact that the minimization of the variational problem is 2.5 times more expensive than the adiabatic (or simplified physics) solution. Another strategy is then proposed to reduce the extra-cost of the physics and also to better account for the non-linearities it introduces.

A "two-update" configuration has been defined, where a first minimization is performed with only the simplified physics from Buizza (1994), followed by a second minimization with improved physics after updating the trajectory at high resolution. The underlying idea is similar to the multi-incremental approach proposed by Veersé et al. (1998). We assume that the minimization will first adjust the larger scales of the atmospheric flow which are correctly described by a model without physics, and then the minimization will adjust the smaller scales which depend more on physical processes. With such configuration, the increase in computing time introduced by the linear physics has been reduced to 50 % in a "40/40" configuration (40 iterations with SP followed by 40 iterations with IP). For few assimilation cycles, it has been checked that the behaviour of the minimization when the linear physics is activated after a first update of the trajectory is very similar to a minimization where the physics is always activated as shown in Table 1. The two update configuration provides a lower value of the cost-function at the beginning of the minimization (the first-guess is thus closer to the observations) and also at the end of the descent process after the observation term is recomputed at high resolution. A "50/20" configuration was finally chosen in order to reach a better convergence during the first minimization. Since the quality control is only activated after 30 simulations, it needs more than 10 iterations to stabilize the convergence with the reduced set of observations (Figure 7a). The reduction of the number of iterations with IP to 20 leads to an extra-cost imposed by the physics of only 25 %. The additional trajectory at high resolution also imposes a 25 % increase with respect to the one outer-loop configuration. The impact of the improved physics on this 4D-Var configuration is evaluated in the next section. Part III will describe a more extensive evaluation against the 3D-Var system (Klinker et al., 1999).

Experiment	Jo(L)	Jo(H)	Jo(FG)	CPU (sec)
1UP SP	40256	45245	86441	21258
2UP IP/IP	40650	44321	85320	61620
2IP SP/IP	40539	44342	85336	37811

TABLE 1. OBSERVATION TERM OF THE COST-FUNCTION FOR AN ASSIMILATION CYCLE (17/02/97 AT 12Z) AND VARIOUS CONFIGURATIONS OF 4D-VAR. JO(H) IS THE OBSERVATION TERM AT HIGH RESOLUTION, JO(L) IS THE OBSERVATION TERM AT LOW RESOLUTION AND JO(FG) IS THE OBSERVATION TERM AT THE BEGINING OF THE MINIMIZATION (FIT TO THE FIRST-GUESS). "1UP SP" IS A ONE UPDATE CONFIGURATION (70 ITERATIONS) WITH SIMPLIFIED PHYSICS, "2UP IP/IP" IS A TWO UPDATE CONFIGURATION WITH 40 ITERATIONS WITH IMPROVED PHYSICS AND 40 ITERATIONS WITH IMPROVED PHYSICS, "2UP SP/IP" IS A TWO UPDATE CONFIGURATION WITH 40 ITERATIONS WITH SIMPLIFIED PHYSICS AND 40 ITERATIONS WITH IMPROVED PHYSICS.

5. EXPERIMENTATION OF 4D-VAR WITH TWO OUTER LOOPS

Three configurations of 4D-Var are tested during a two-week winter period (1 to 14 February 1997) using the operational 3D-Var as a control :

- 4D-Var one-update SP

- 4D-Var two-updates SP

- 4D-Var two-updates with IP in the second minimization

We compare the performance of these three versions of 4D-Var in order to evaluate the impact of both the "two outer-loops" configuration and of the physics. The extra-tropical scores are presented on Figure 9 in terms of anomaly correlation for the geopotential at 1000 hPa. The impact of including physical processes is rather neutral, whereas going from one to two-updates outer loops is slightly detrimental in the Southern Hemisphere around day 3. A more extended comparison of 4D-Var with one-outer loop and 4D-Var with two-outer loops over 56 days has demonstrated that this feature is not systematic. The neutral impact of the linear physics over mid-latitudes can be understood by examining the RMS errors of short range forecasts differences between the various systems. Differences of 12-hour forecast errors for the temperature at 850 hPa are compared between 3D-Var and 4D-Var on Figure 10a and between 4D-Var adiabatic and 4D-Var with physics on Figure 10b. The differences between 3D-Var and 4D-Var mostly take place over the Atlantic and Pacific oceans along the storm tracks. Although some differences are present with the inclusion of the physics, they are located over Siberia above 60°N which is not a sensitive region for the growth unstable perturbations. Therefore, these short-range forecast differences are not likely to influence the medium range.

In terms of weather parameters, the agreement with observations from SYNOP stations is slightly better over Europe when the linear physics is included in 4D-Var. For instance, the fit to observed 2-metre temperature, which is improved by 4D-Var one outer-loop without physics compared with 3D-Var, is further improved when adding the physics in the second outer-loop (Figure 11).

The inclusion of the linear physics has the largest impact on the analysis of specific humidity. The zonal mean increments of specific humidity averaged over the two-week period show a global moistening of the lower tropical troposphere and a drying in mid-latitudes with both configurations (Figure 12). The vertical profile of the increments is imposed by the statistics of background error for specific humidity derived from the NMC method described by Rabier et al. (1998b) and Bouttier et al. (1997). The standard deviations of forecast errors are maximum around 850 hPa where the increments are the largest. Around level 28, vertical correlations are very small leading to minimum values of increments. There is a significant reduction of the increments in the tropical belt, both in the boundary layer and above between 4D-Var with physics and standard 4D-Var. As shown before, the inclusion of physical processes weakens the amplification of initial perturbations (except in rainy areas where no observations are taken into account). This effect is more dominant for specific humidity since no diabatic processes are applied with the simplified physics (dry vertical diffusion). The fit to the data is therefore more difficult when the improved physics in included in 4D-Var. It is important to underline that mean increments of specific humidity were systematically larger in the standard 4D-Var system than in 3D-Var, explaining part of the worse performance of 4D-Var in the tropics (Rabier et al., 1998a).

The direct consequence of a drier initial atmospheric state when introducing the physics is a significant reduction of the spin-down for precipitation during the first day of the forecasts as shown by Figure 13 where the time evolution of total precipitation in the tropical belt (between 30°S and 30°N) averaged of the 14 forecasts is presented. The tropical circulation being strongly driven by the distribution of diabatic heating, moisture analysis has a direct influence on the quality of wind forecasts. The short-range tropical wind scores are improved with the inclusion of physical processes, whereas the impact of the two-update configuration is almost neutral. The improvement is larger at 850 hPa than at 200 hPa (Figure 14) in agreement with the stronger impact of the linear physics on the time evolution of increments of specific humidity in the tropical belt. Although the inclusion of physics is beneficial for the analysis of humidity, the fact that less

weight should be given to the observations in the assimilation indicates that other improvements need to be brought to the system both on the tuning of observation errors and on the statistics of forecast errors (which are currently global and univariate).

The comparison between the baseline 4D-Var and the 4D-Var with two outer-loops (with physics in the second outer-loop) has been performed on a total of eight weeks. These include the periods 1 to 14 February 1997, 26 August to 6 September 1995, 15 to 28 January 1997 and 27 June to 10 July 1997. The scores over the Northern and Southern Hemispheres are marginally positive, with a larger positive signal over Europe. The scatter between 4D-Var and 4D-Var with physics is very small in the short-range and the fit of the background fields to the data very similar. The overall clearest improvement is seen in the Tropics for the 850 hPa wind field, similar to the one in Figure 14 for one two-week period.

6. CONCLUSIONS

A configuration of the incremental 4D-Var developed at ECMWF and described in Part I (Rabier et al., 1999) has been evaluated by including physical processes in the tangent-linear and adjoint versions of the model. A comprehensive package of linear physics has been described and simplifications with respect to the operational physics explained. The linear physics has been evaluated by comparing the time evolution of analysis increments produced by the tangent-linear model with differences between two non-linear integrations. The inclusion of the linear physics improves the behaviour of the tangent-linear model with respect to the non-linear model. The improvement for a T63L31 version of the ECWMF model over a 6-hour time window with respect to a simple vertical diffusion scheme has been illustrated for both surface wind and specific humidity. Singular vectors have been computed with linear physics over 6 hours in the extra-tropics. Amplification rates are generally smaller with improved physics, except in areas where latent heat release takes place. The inclusion of improved physics in 4D-Var has lead to a better consistency between the minimization at high and low resolutions. The expensive cost of the linear physics has required to define a new 4D-Var configuration with two outer-loops where a first minimization without physics (50 iterations) is followed by a second minimization with physical processes activated (20 iterations). For such configuration, the increase in computational cost is 50 % with respect to the one update configuration presented in Part I (half of it comes from the physics and the other half comes from the extra-trajectory computation). Improvements of the forecasts have been shown over Europe for weather parameters and over the Tropics for wind scores (by a reduction of the spin-down in precipitation). This 4D-Var configuration with two updates including improved physics in the second outer loop is extensively evaluated against the operational 3D-Var system in Part III (Klinker et al, 1999).

REFERENCES

Andersson, E., J. Haseler, P. Unden, P. Courtier, G. Kelly, D. Vasiljevic, C. Brankovic, C. Cardinali, C. Gaffard, A. Hollingsworth, C. Jakob, P. Janssen, E. Klinker, A. Lanzinger, M. Miller, F. Rabier, A. Simmons, B. Strauss, J.-N. Thépaut and P. Viterbo, 1998: The ECMWF implementation of three-dimensional variational assimilation (3D-Var). Part III: Experimental results. *Q. J. R. Meteorol. Soc.*, **124**, 1831-1860.

Betts, A.K., 1997 : The parameterization of deep convection: a review. ECMWF Workshop on new insights and approaches to convective parametrization, pages 166-188. ECMWF, Shinfield Park, Reading (U.K.), 4-7 November 1996

Blackadar, A.K., 1962: The vertical distribution of wind and turbulent exchange in a netral atmosphere. *J. Geophys. Res.*, 67, 3095-3102

Bouttier, F., J. Derber and M. Fisher, 1997: The 1997 revision of the Jb term in 3D/4D Var. ECMWF Technical Memorandum No 238, 54 pp.

Buizza, R., 1994: Sensitivity of optimal unstable structures. *Quart. J. Roy. Meteor. Soc.*, 120, 429-451

Courtier, P., J.-N. Thépaut and A. Hollingsworth, 1994 : A strategy for opertional implementation of 4D-Var using an incremental approach. *Quart. J. Roy. Meteor. Soc.*, **120**, 1367-1387

Courtier, P., E. Andersson, W. Heckley, J. Pailleux, D. Vasiljevic, M. Hamrud, A. Hollingsworth, F. Rabier and M. Fisher, 1998 : The ECMWF implementation of the three-dimensional variational assimilation (3D-Var). Part I: Formulation. *Q. J. R. Meteorol. Soc.*, **124**, 1783-1807

Ehrendorfer, M., R.M. Errico and K.D. Raeder, 1998 : Singular-vector purturbation growth in a primitive-equation model with moist physics. *J. Atmos. Sci.* (accepted for publication)

Errico, R.M. and K.D. Raeder, 1998: An examination of the accuracy of the linearization of a mesoscale model with moist physics. *Q. J. R. Meteorol. Soc.*, (accepted for publication)

Gregory, D. and M. Miller, 1989: A numerical study of the parametrization of deep tropical convection. *Quart. J. Roy. Meteor. Soc.*,115, 1209-1241

Janiskova, M., J.-N. Thépaut and J.-F. Geleyn, 1998: Simplified and regular physical parametrizations for incremental four-dimensional variational assimilation. *Mon. Weather Rev.* (accepted for publication)

Klinker, E., F. Rabier and R. Gelaro, 1998: Estimation of key analysis errors using the adjoint technique. *Q. J. R. Meteorol. Soc.*, **124**, 1909-1934

Klinker, E, F. Rabier, G. Kelly, J.-F, Mahfouf and M. Fisher, 1999: The ECMWF operational implementation of four dimensional variational assimilation. Part III: Experimental results and diagnostics with operational configuration. *Q. J. R. Meteorol.* (submitted)

Lacarra, J.-F. and O. Talagrand, 1988 : Short-range evolution of small perturbations in a barotropic model, *Tellus*, **40A**, 81-95

Lott, F., and M.J. Miller, 1997: A new subgrid-scale drag parametrization: Its formulation and testing. *Q. J. R. Meteorol. Soc.*,123,101-127

Louis, J.-F., M. Tiedtke and J.-F. Geleyn, 1982: A short history of the operational PBL parametrization at ECMWF. ECMWF Workshop on boundary layer parametrization, pages 59-79. ECMWF, Shinfied Park, Reading (U.K.), November 1981.

Mahfouf, J.-F., R. Buizza and R.M. Errico, 1996: Strategy for including physical processes in the ECMWF variational data assimilation system. ECMWF Workshop on non-linear aspects of data assimilation, pages 595-632, Shinfield Park, Reading (U.K.), ECMWF, 9-11 September 1996.

Mahfouf, J.-F., 1998 : Influence of physical processes on the tangent-linear approximation, *Tellus* (accepted for publication)

Morcrette, J.-J., 1990 : Impact of changes to the radiation transfer parametrization plus cloud optical properties in the ECMWF model. *Mon. Weather Rev.*, **118**, 847-873

Rabier, F., J.-N. Thépaut and P. Courtier, 1998a : Extended assimilation and forecast experiments with a four-dimensional variational assimilation system. *Q. J. R. Meteorol. Soc.*, **124**, 1861-1887

Rabier, F., A. McNally, E. Andersson, P. Courtier, P. Unden, J. Eyre, A. Hollingsworth and F. Bouttier, 1998b: The ECMWF implementation of three-dimensional variational assimilation (3D-Var). Part II: Structure functions. *Q. J. R. Meteorol. Soc.*, **124**, 1809-1829

Rabier, F., H. Jarvinen, E. Klinker, J.-F. Mahfouf and A. Simmons, 1999: The ECMWF operational implementation of four dimensional variational assimilation. Part I: Experimental results with simplified physics. *Q. J. R. Meteorol. Soc.* (submitted)

Thuburn, J., 1994: Stratospheric modelling within UGAMP. ECMWF Workshop on stratosphere and numerical weather prediction, pages 193-212, Shinfield Park, Reading (U.K.), ECMWF, 15-17 November 1993

Tiedtke, M., 1989: A comprehensive mass-flux for cumulus parameterization in large-scale models. *Mon. Weather Rev.*, **117**, 1779-1800

Tiedtke, M., 1993: Representation of clouds in large-scale models. *Mon. Weather Rev.*, **121**, 3040-3061

Tsuyuki, T., 1996: Variational data assimilation in the tropics using precipitation data. Part II: 3D model. *Mon. Weather Rev.*, **124**, 2545-2561

Veersé, F. and J.-N. Thépaut, 1998: Multiple-truncation incremental approach for four-dimensional variational data assimilation. *Q. J. R. Meteorol. Soc.*, **124**, 1889-1908

Zou, X., 1996: Tangent-linear and adjoint of "on-off" processes and their feasibility for the use in 4-dimensional variational data assimilation. *Tellus*, **49A**, 3-31

Zupanski, D., 1993 : The effects of discontinuities in the Betts-Miller cumulus convection scheme on four-dimensional variational data assimilation. *Tellus*, **45A**, 511-524.

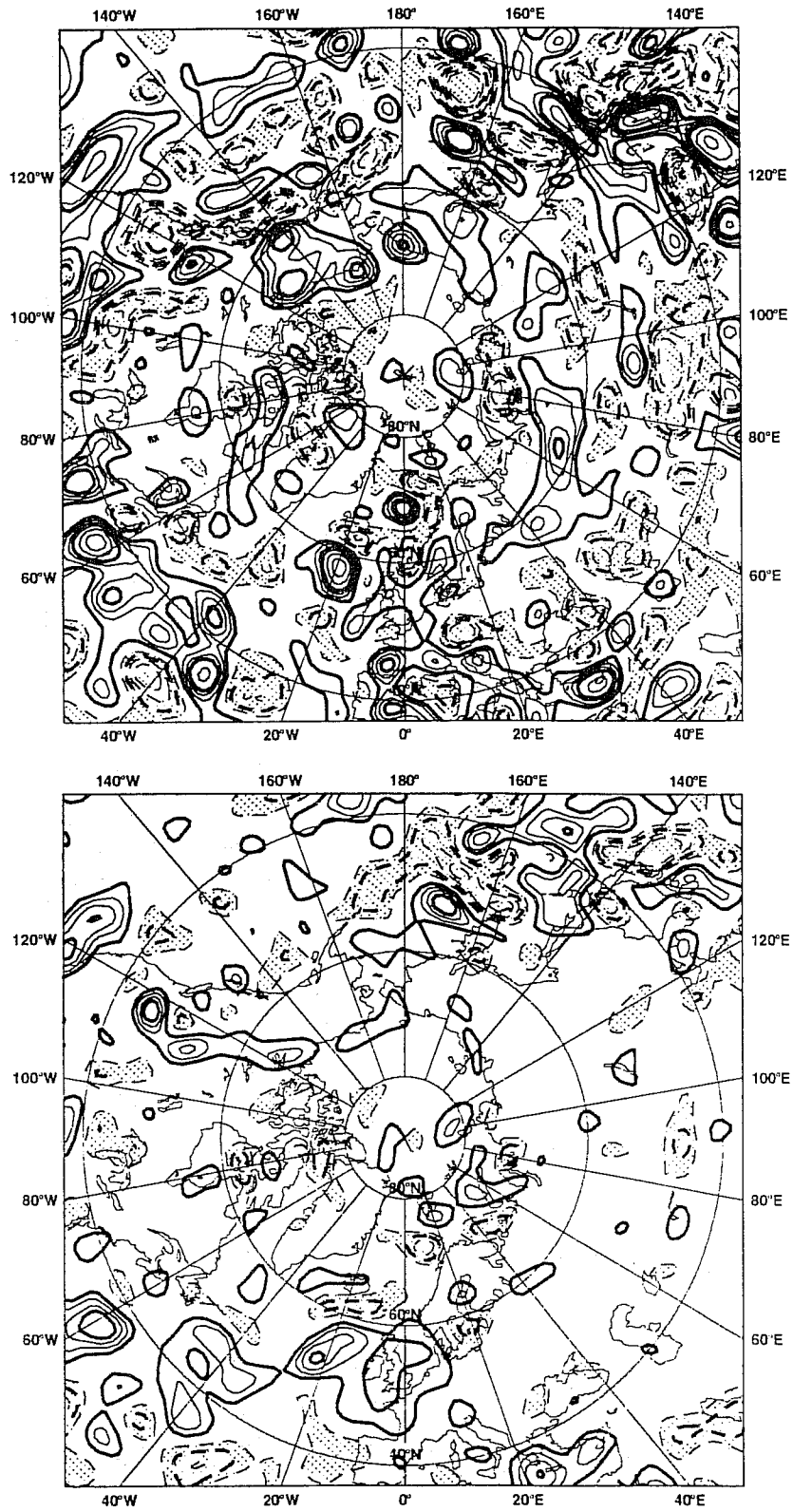

Figure 1: Analysis increments of the zonal wind at model level 31 (~30 metres) for 5 December 1996 at 00Z (upper panel) and after a 6-hour evolution obtained from the difference between two non-linear integrations with full physics (lower panel). The isoligns are plotted every 0.5 ms^{-1}.

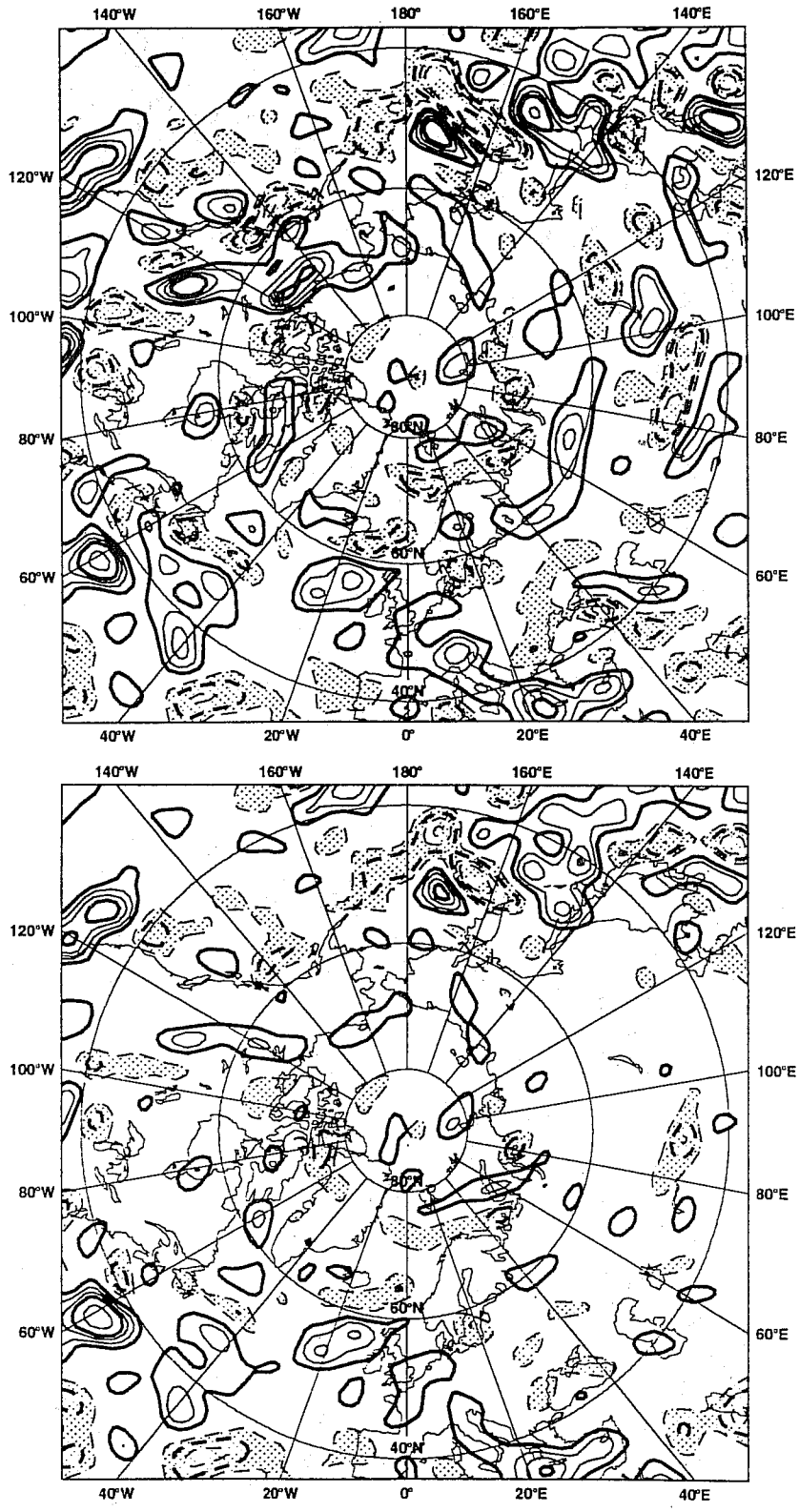

Figure 2: Evolution of analysis increments for zonal wind at model level 31 (~30 metres) during 6 hours produced with a tangent-linear model with simplified physics (upper panel) and a tangent-linear model with improved physics (lower panel). The isoligns are plotted every 0.5 ms^{-1}

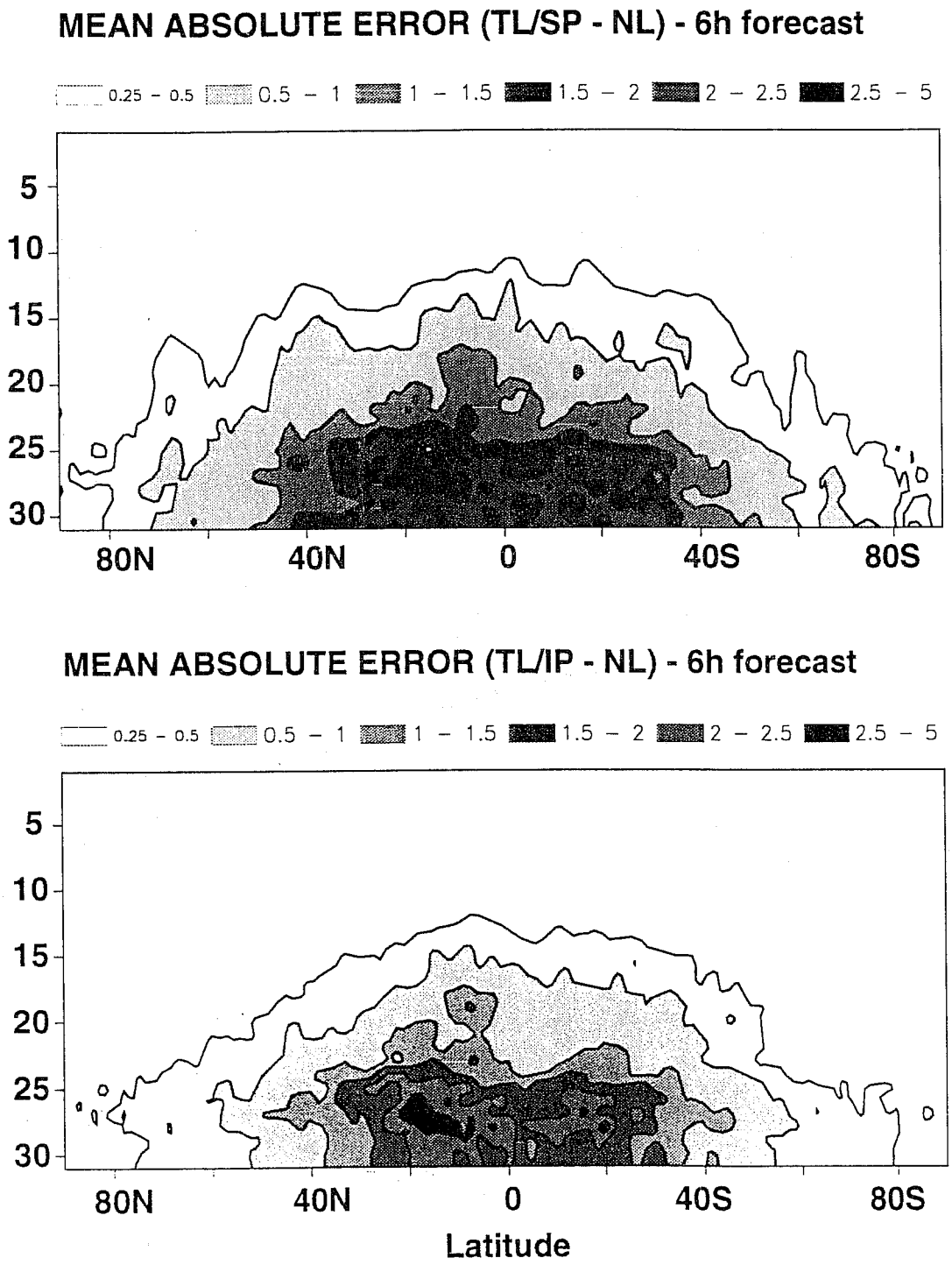

Figure 3: Mean absolute errors of specific humidity increments evolved during 6 hours using tangent-linear models with simplified physics (upper panel) and improved physics (lower panel). Errors are computed with respect to pairs of non-linear integrations with full physics.

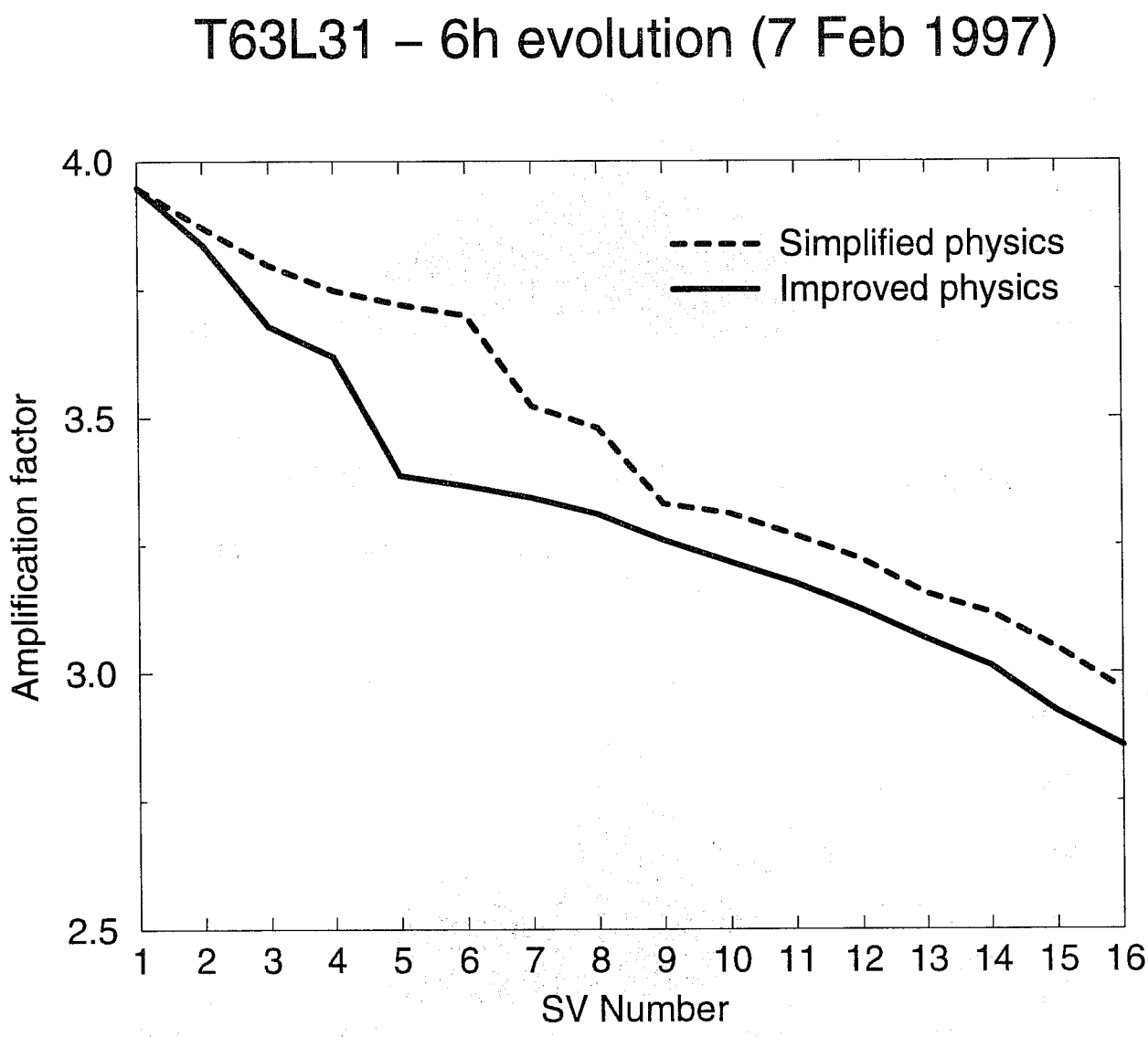

Figure 4: Amplification factors of singular vectors computed with simplified physics (dashed) and improved physics (solid) for an optimization time interval of 6 hours.

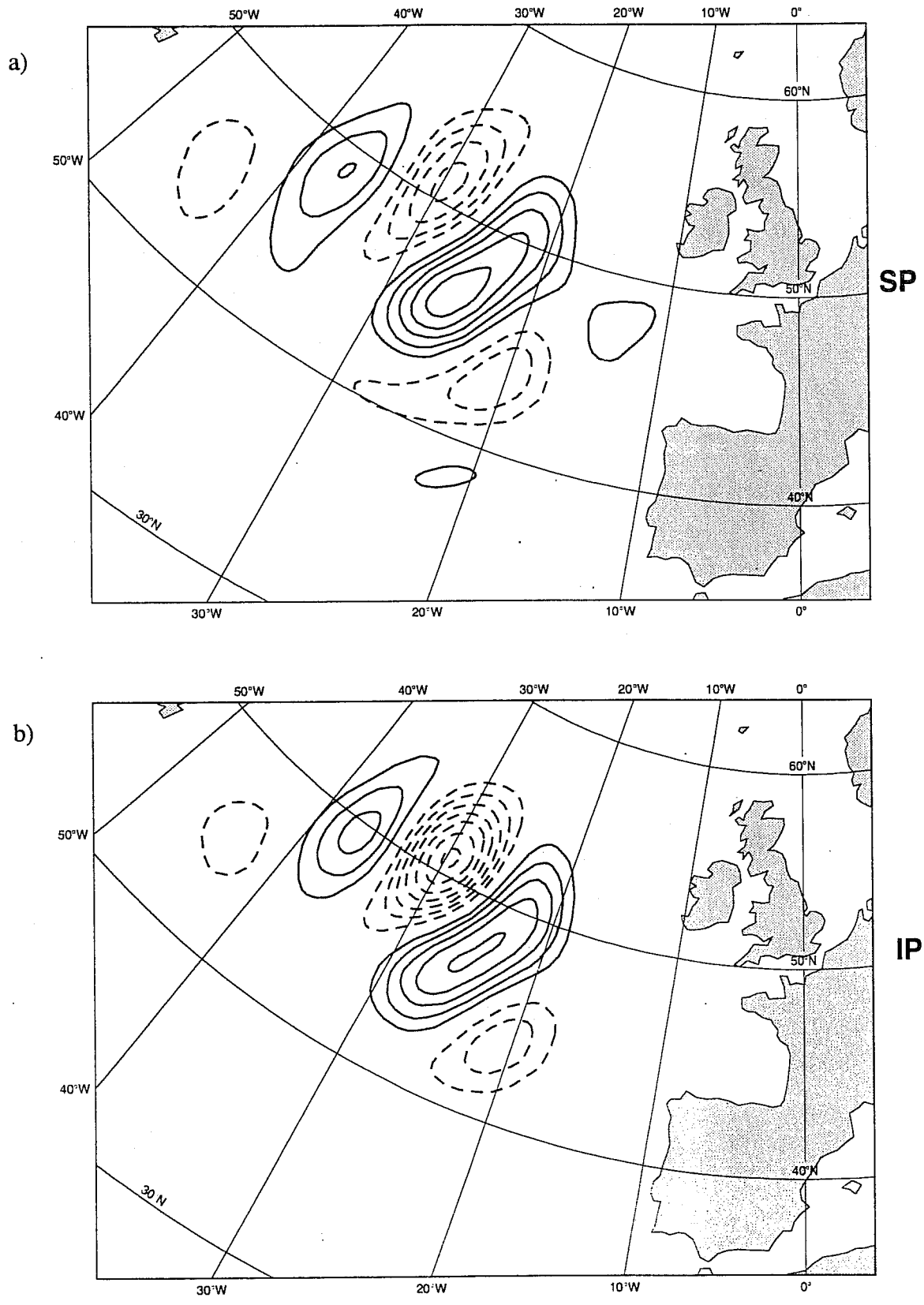

Figure 5: First singular vector at model level 15 (~500 hPa) for temperature after a 6 hour evolution from 07 February 1997 at 12Z computed with simplified physics (upper panel) and with improved physics (lower panel).

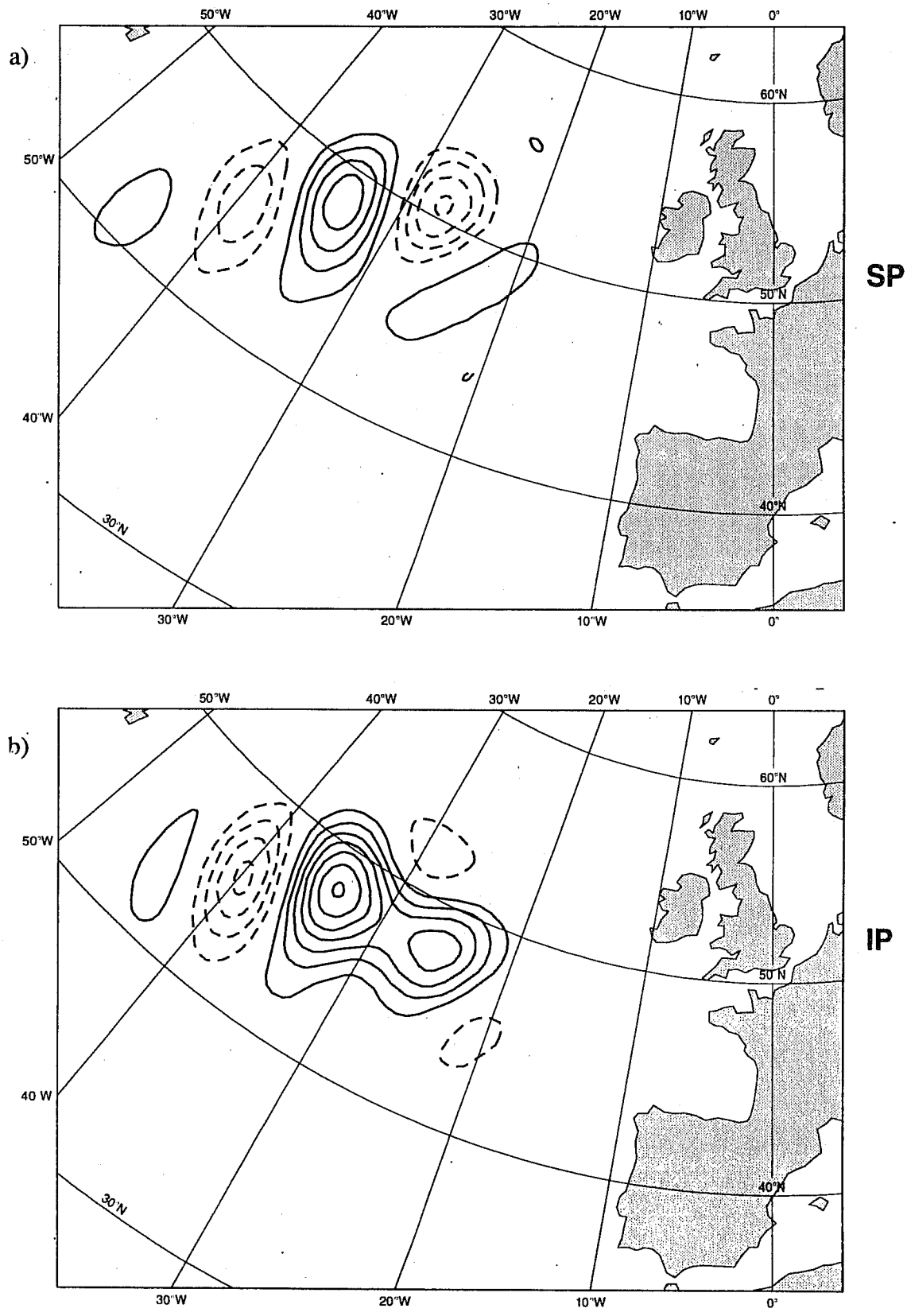

Figure 6: First singular vector at model level 22 (~700 hPa) for specific humidity after a 6 hour evolution from 07 February 1997 at 12Z computed with simplified physics (upper panel) and with improved physics (lower panel).

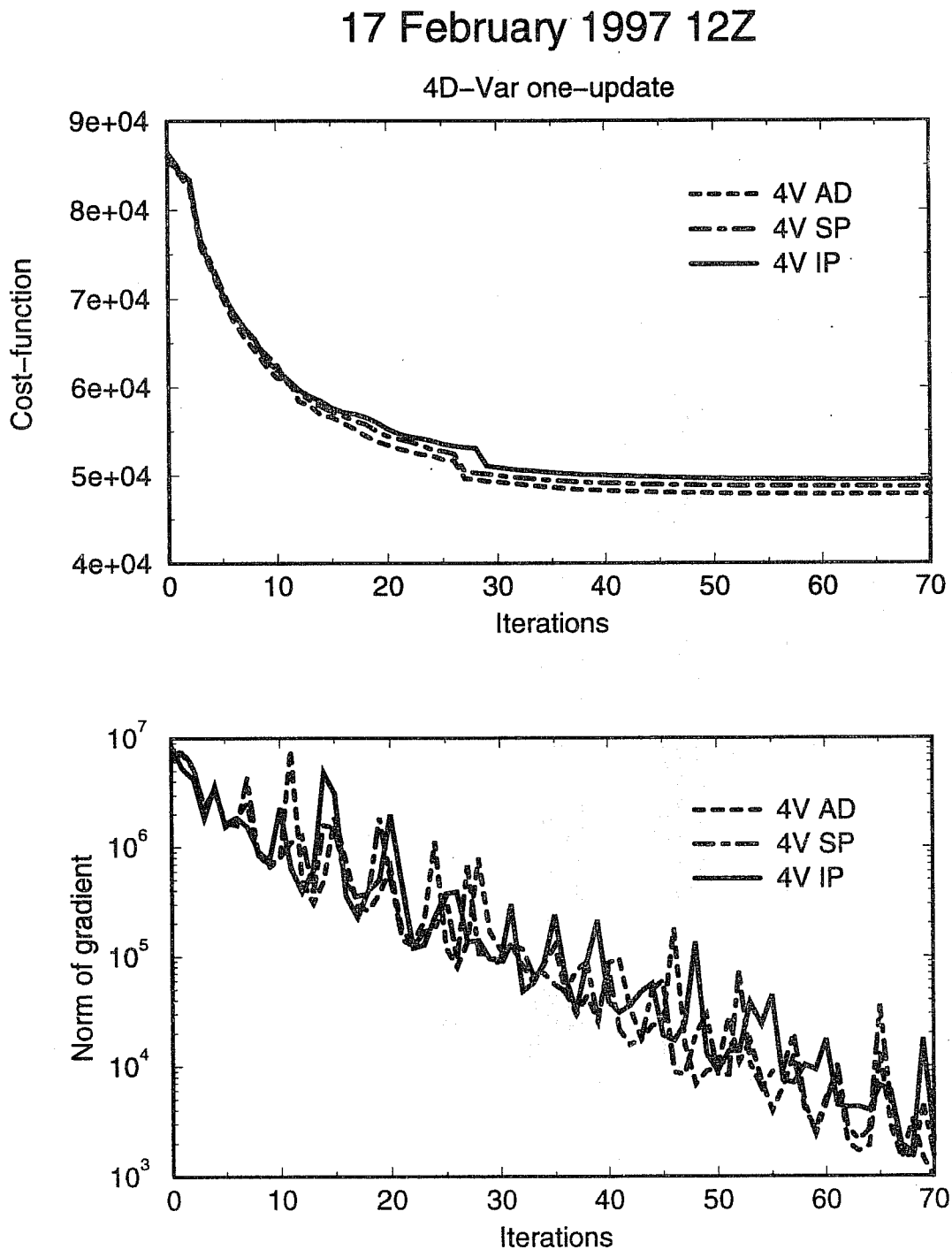

Figure 7: Cost-function and its gradient during the minimization process of an assimilation cycle (17/02/97 at 12 Z) for three configurations of the 4D-Var system. "4V AD" is a 4D-Var one update adiabatic, "4V SP" is a 4D-Var one update with simplified physics, "4V IP" is a 4D-Var one update with improved physics.

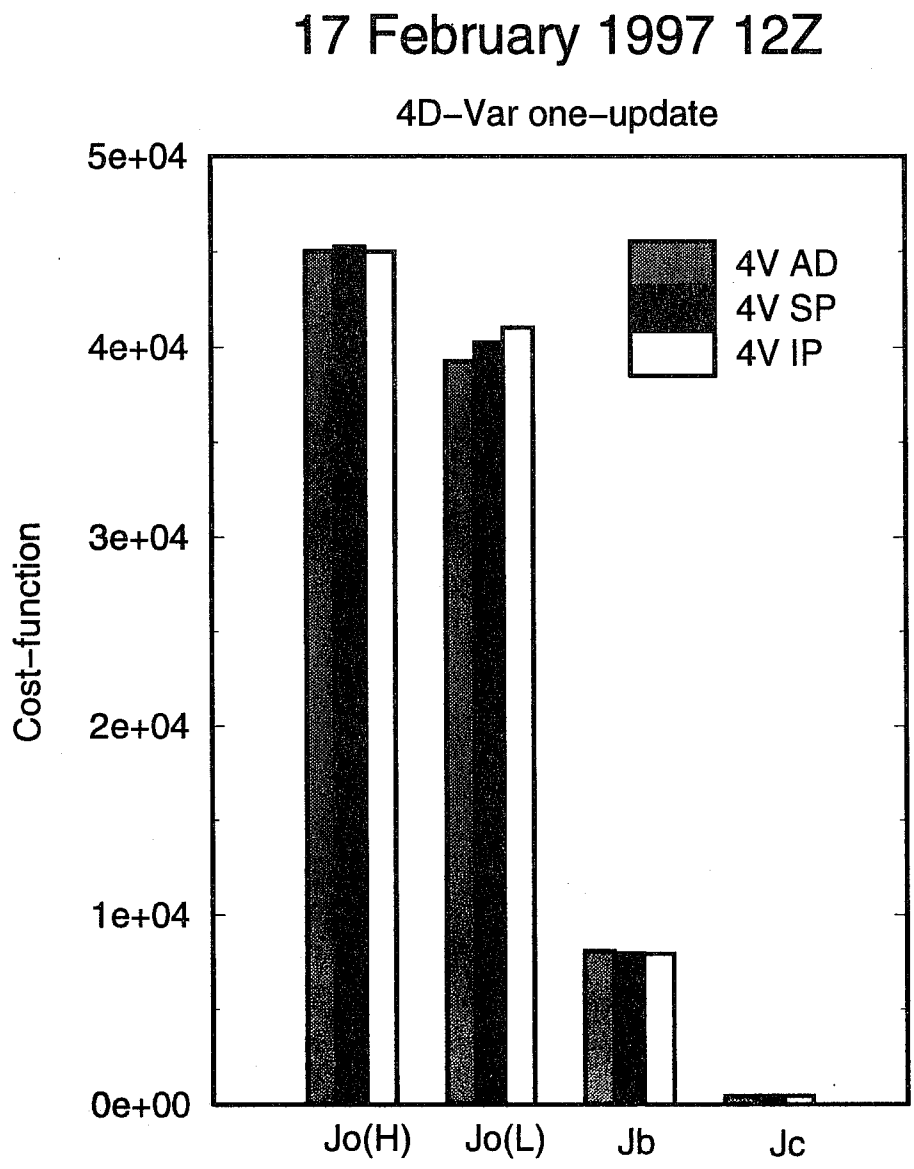

Figure 8: Contributions to the total cost-function for three configurations of the 4D-Var system on the 17/02/97 at 12Z. "4V AD" is a 4D-Var one update adiabatic, "4V SP" is a 4D-Var one update with simplified physics, "4V IP" is a 4D-Var one update with improved physics. Jo(H) is the observation term computed at high resolution, Jo(L) is the observation term computed at low resolution, Jb is the bakcground term and Jc the penalty term.

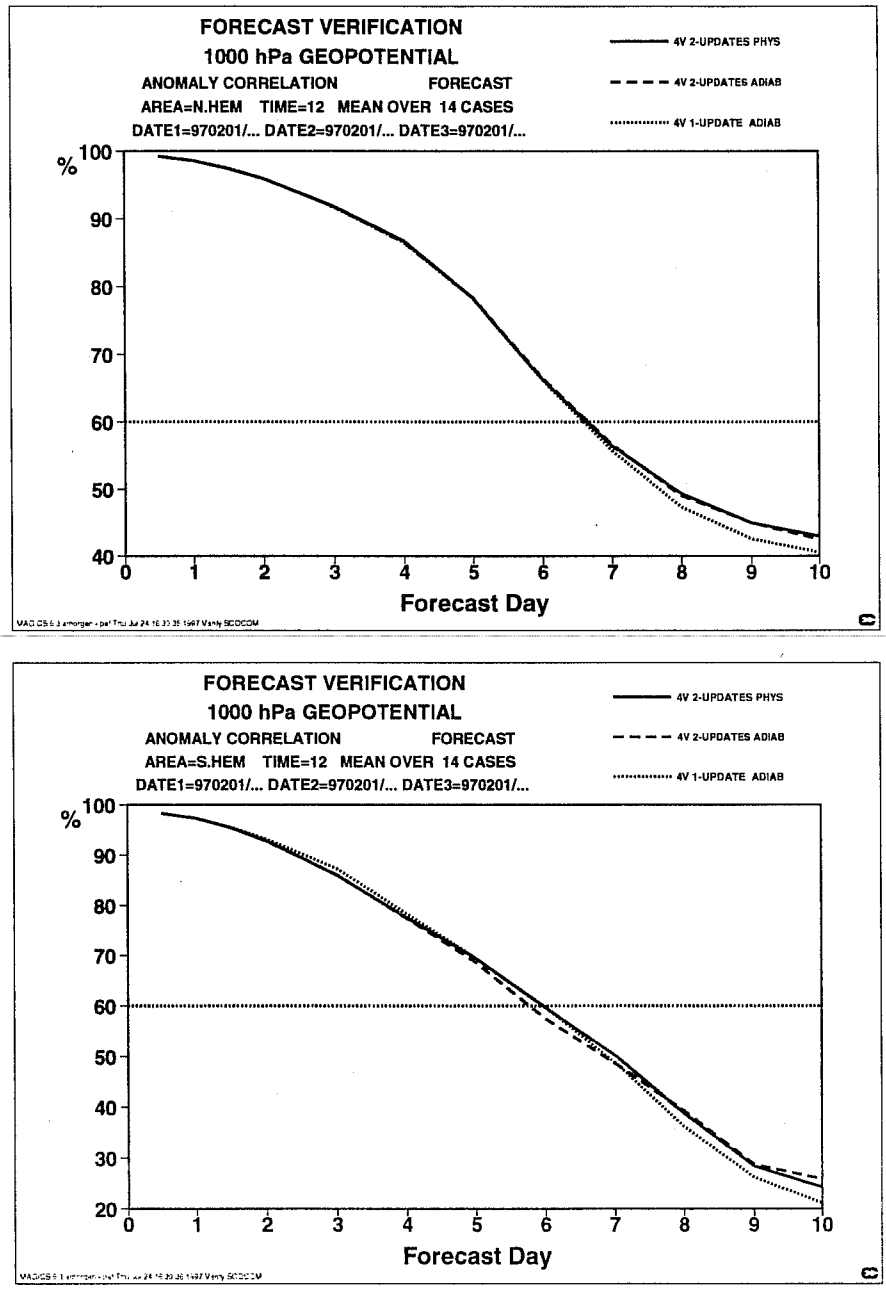

Figure 9: Anomaly correlation for the geopotential at 1000 hPa averaged over 14 forecasts (1 to 14 February 1997) issued from 4D-Var one update with simplified physics (dotted), 4D-Var two updates with simplified physics (dashed) and 4D-Var two updates with improved physics (solid). Top : Northern hemisphere, bottom : Southern Hemisphere.

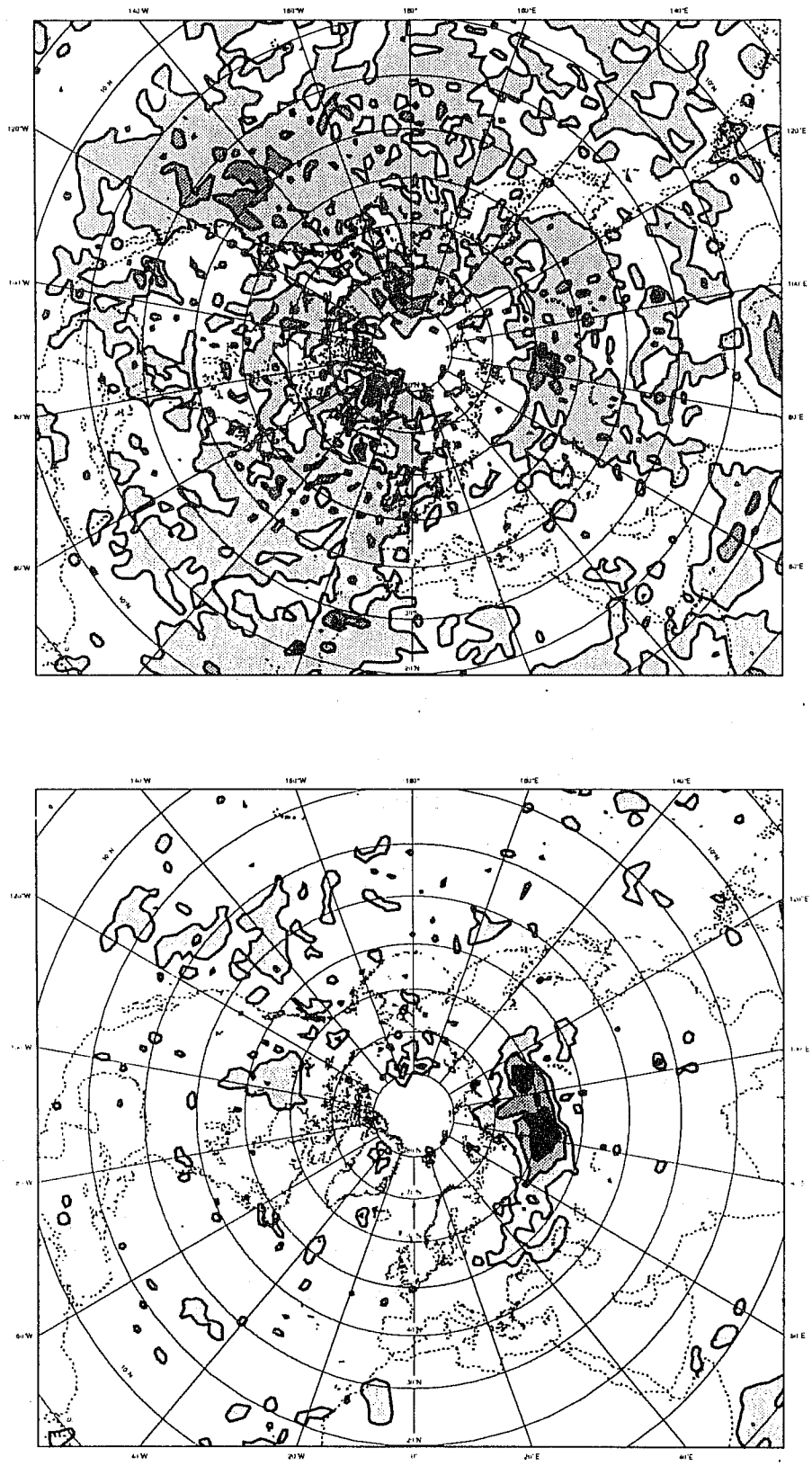

Figure 10: Root mean square differences of 12-hour forecasts of temperature at 850 hPa between 4D-Var with simplified physics and 3D-Var (upper panel) and 4D-Var with improved physics and 4D-Var with simplified physics (lower panel)

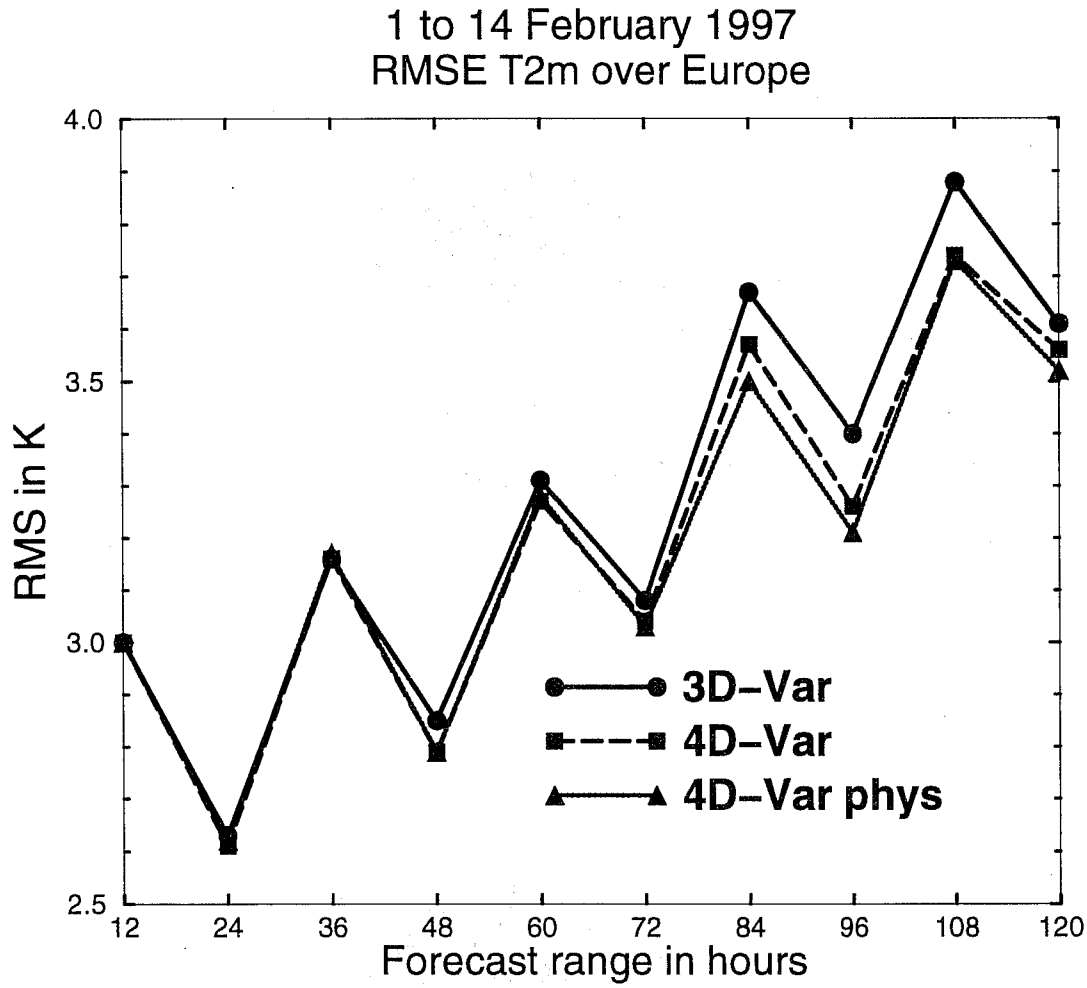

Figure 11: Root mean square of the difference between forecasts from 4D-Var with simplified physics (squares) and observations, forecasts from 4D-Var with improved physics and observations (triangles) and forecasts from 3D-Var and observations (circles) averaged over 14 days over Europe for the 2-metre temperature.

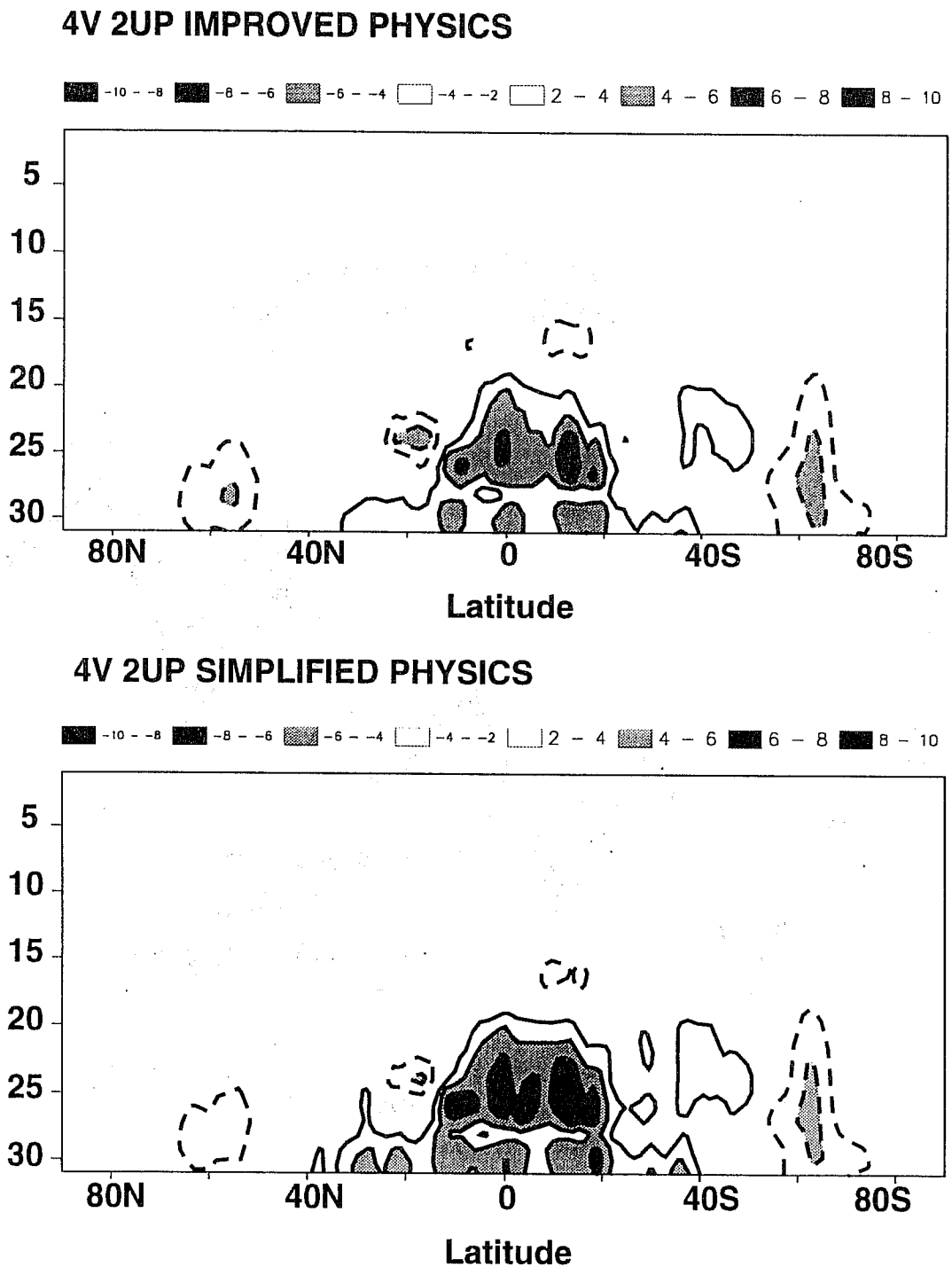

Figure 12: Mean zonal analysis increments for specific humidity (unit is 0.01 gkg^{-1}) averaged over a two-week period (01/02/97 - 14/02/97). Top: 4D-Var two-updates with improved physics, bottom: 4D-Var two-updates with simplified physics

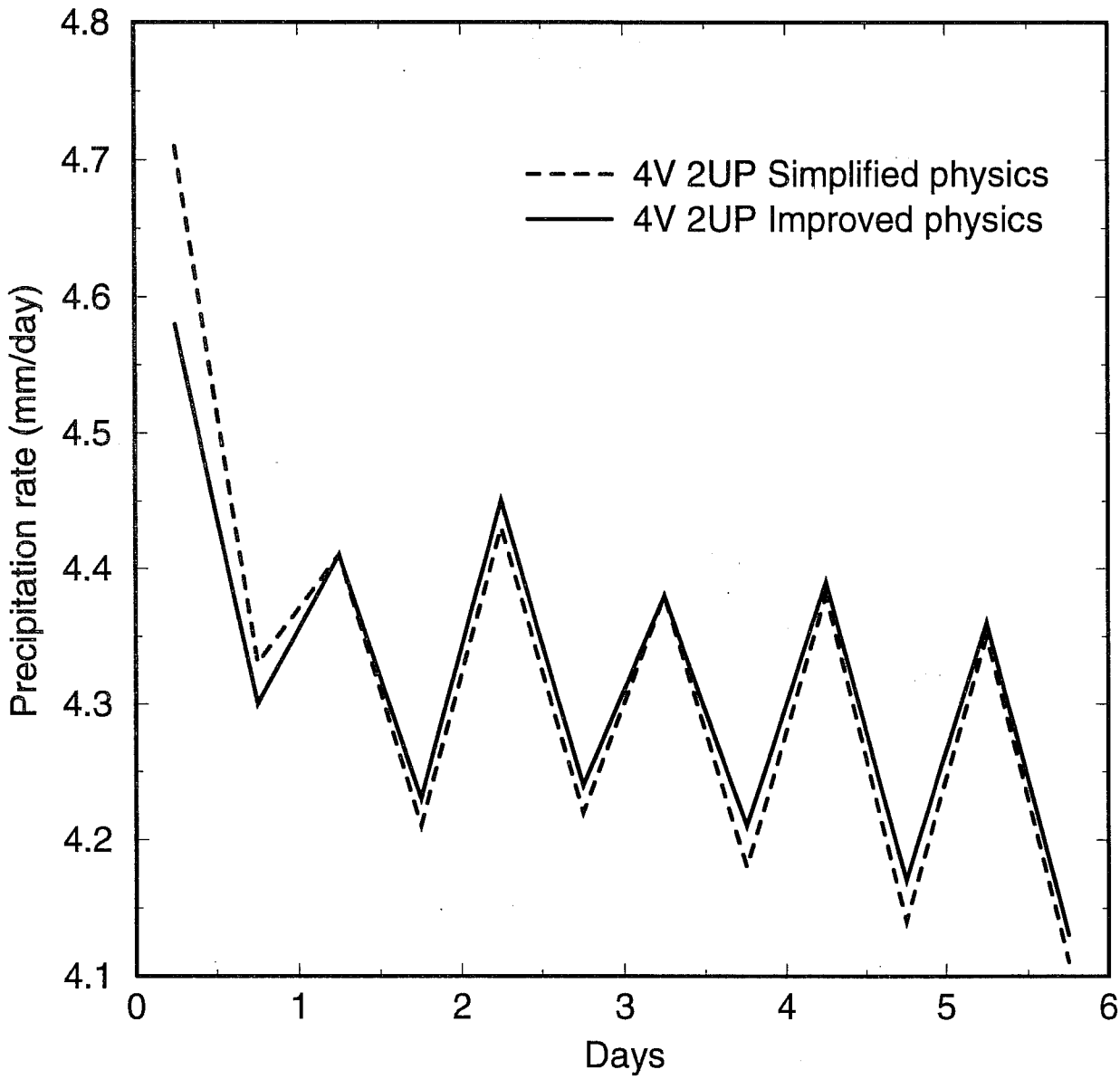

Figure 13: Time evolution of global precipitation in the tropical belt [30°S, 30°N] averaged over 14 forecasts issued from 4D-Var assimilation two-updates with simplifed and improved physics.

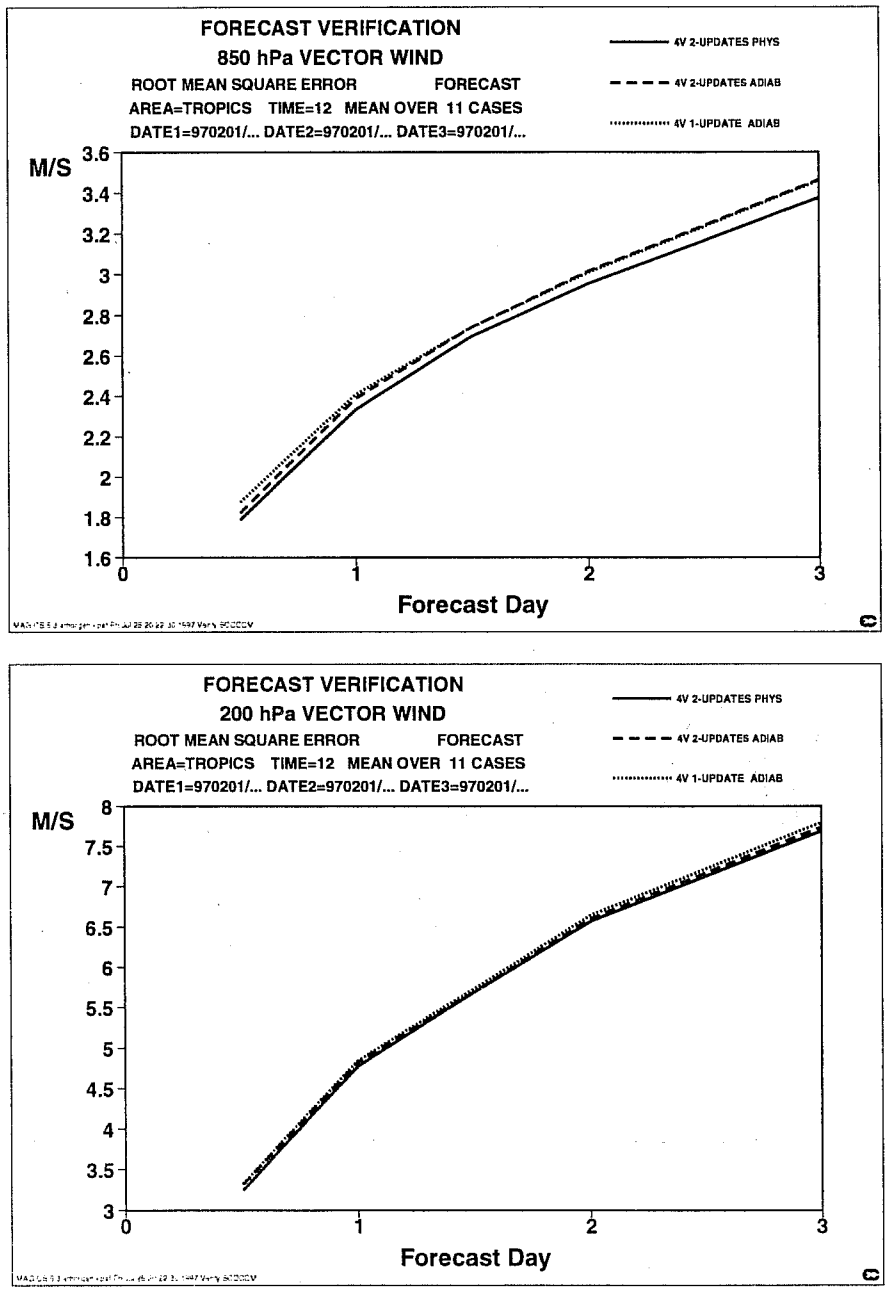

Figure 14: Tropical wind scores verified against own analysis at 850 and 200 hPa averaged over 11 forecasts from 4D-Var assimilation one-update with simplified physics (dotted), two-updates with simplified physics (dashed) and two-updates with improved physics (solid)